Fly ash based geopolymeric foams using silica fume as pore generation agent. Physical, mechanical and acoustic properties

***Y. Luna-Galiano, C. Leiva, C. Arenas, C. Fernández-Pereira**

University of Seville, School of Engineering, Chemical and Environmental Engineering Department, Camino de los Descubrimientos s/n 41092, Seville (Spain), (0034-954481180, Fax: 0034-954486082, yluna@us.es)

Abstract

The aim of this work is the development of a porous geopolymeric foam with sound absorbing properties using silica fume as the pore generation agent. The samples were manufactured using a coal combustion fly ash as source material for the geopolymerization reaction, an alkaline solution as activating solution and silica fume as pore forming agent. Three parameters were studied: silica fume proportion (0, 20 and 40 wt%), activating solution (potassium silicate and potassium hydroxide) and setting temperature (40 and 70 ºC). Once the samples were prepared, the experimental study of the most important physical, mechanical and acoustic features were carried out. The increase in the proportion of silica fume in the mixture and setting temperature produced a reduction in setting time and a raise of open void porosity, reducing the compressive strength at 28 days up to a half but increasing the sound absorption. The influence of activating solution in open porosity and sound absorbing properties was not very important.

Keywords: fly ash, foam geopolymer, pore generation, open porosity, mechanical properties, acoustic properties

1. Introduction

Geopolymers are considered an eco-friendly construction material [1]. This material exhibits great potential in several applications [2]: as binder agent in the stabilization/solidification of industrial wastes [3-6], as fire resistant material in construction [7-10], as hydraulic road binder [11], as acoustic concrete [12-13], among others [14]. The construction field is where geopolymers can compete with cement products [15] due to a large number of useful/beneficial properties: high compressive strength and structural integrity [16], resistance to acids and salts [16, 17], low permeability [16], and medium-high density [18]. The challenge of the current work is to study and evaluate pore generation in a fly ash based geopolymer in order to manufacture a foam product. A foam product is considered a type of lightweight material that consists of a binder with a high degree of void space [19]. There are two traditional methods of pore generation in a mortar [19]: by endogenous gas generation, which can be achieved by mixing gas-releasing agents such as H_2O_2 [20], aluminium [21, 22] or silica [23, 24], or by introducing a very large volume fraction of air bubbles, normally using an organic foaming agent (surfactants) [20, 25, 26]. Silicon, in the form of silica fume, was used to generate pores in this work. In general, a reactive metal powder (Si) reacts with water and hydroxide in an alkaline environment producing bubbles of hydrogen gas [19]. These bubbles attempt to escape into the air from the geopolymer paste producing the expansion of the geopolymer mortar [27] and generating the porous structure. Silica fume is defined as an inorganic by-product from the metallurgical industry [28]. Several studies have been carried out in which silica fume is added to a metakaolin based geopolymer [24, 29, 30] in order to generate a foam. Prud´homme et al., [23, 24] studied the effect of silica fume content and temperature in the microstructure and porosity of geopolymer foam. Henon [30] concluded that the synthesis of the product and porosity depend to a great extent on the temperature (range 25-70 ºC). In his study, geopolymer foams with macroporosities in the range 05-1.6 mm were developed. Thermal conductivities of 0.12-0.33 W/(mK) for porosities of 65-85 % were obtained. Papa et al., [29]

obtained macroporous structures with roughly rounded pores and a total porosity of about 80%, thermal conductivities of around 0.16 W/(mK) and acoustic behaviour.

In the current work, fly ash based geopolymers have been prepared adding silica fume in different proportions in order to evaluate the physical, mechanical and acoustical properties of the final geopolymeric foam. Two activating solutions and setting temperatures have also been evaluated. In summary, a dual environmental design has been reached: to recycle industrial by-products produced in large amounts and to develop an acoustic absorbing material in order to reduce noise pollution levels.

2. Materials and methods

2.1 Materials

A low calcium fly ash (FA) (ASTM class F [31]) from a coal combustion power plant (Los Barrios, Spain) was used as the geopolymeric precursor. The silica fume (SF) used in this work was supplied by the Sika© company. Chemical composition of the fly ash and the silica fume (Table 1) was determined after chemical attack and dissolution at 750 ºC (ASTM D-3682-78) [32] using atomic absorption spectroscopy. The specific gravity, in accordance with EN 1097-7 [33], was also determined in the fly ash and silica fume (Table 1).

Table 1. Characteristics of fly ash and silica fume

	Moisture (%)	LOI 750ºC	Chemical composition (wt %)							Specific gravity (g/cm^3)
			Fe_2O_3	CaO	MgO	SiO_2	Al_2O_3	Na_2O	K_2O	
FA	0,05	3,32	5,86	3,94	1,84	63,9	21,5	0,68	1,67	1,93
SF	0.03	1,48	0,5	0,51	0,39	96,7	0,43	0,2	0,79	2,04

High SiO_2 and Al_2O_3 contents were observed in FA. The silica fume was practically SiO_2, and its specific gravity (2.04 g/cm^3) was similar to the fly ash (1.93 g/cm^3). Amorphous contents of both

materials were determined after the X-ray powder diffraction (XRD) analysis using DIFFRAC.EVA software. Amorphous content of FA and SF were 44.1 % and 67.1 %, respectively.

The particle size distribution of both materials was determined using a laser diffraction granulometer provided by Micromeritics, which is equipped with an optical system and data acquisition software. The results are shown in Figure 1.

Figure 1. Particle size distribution of fly ash and silica fume

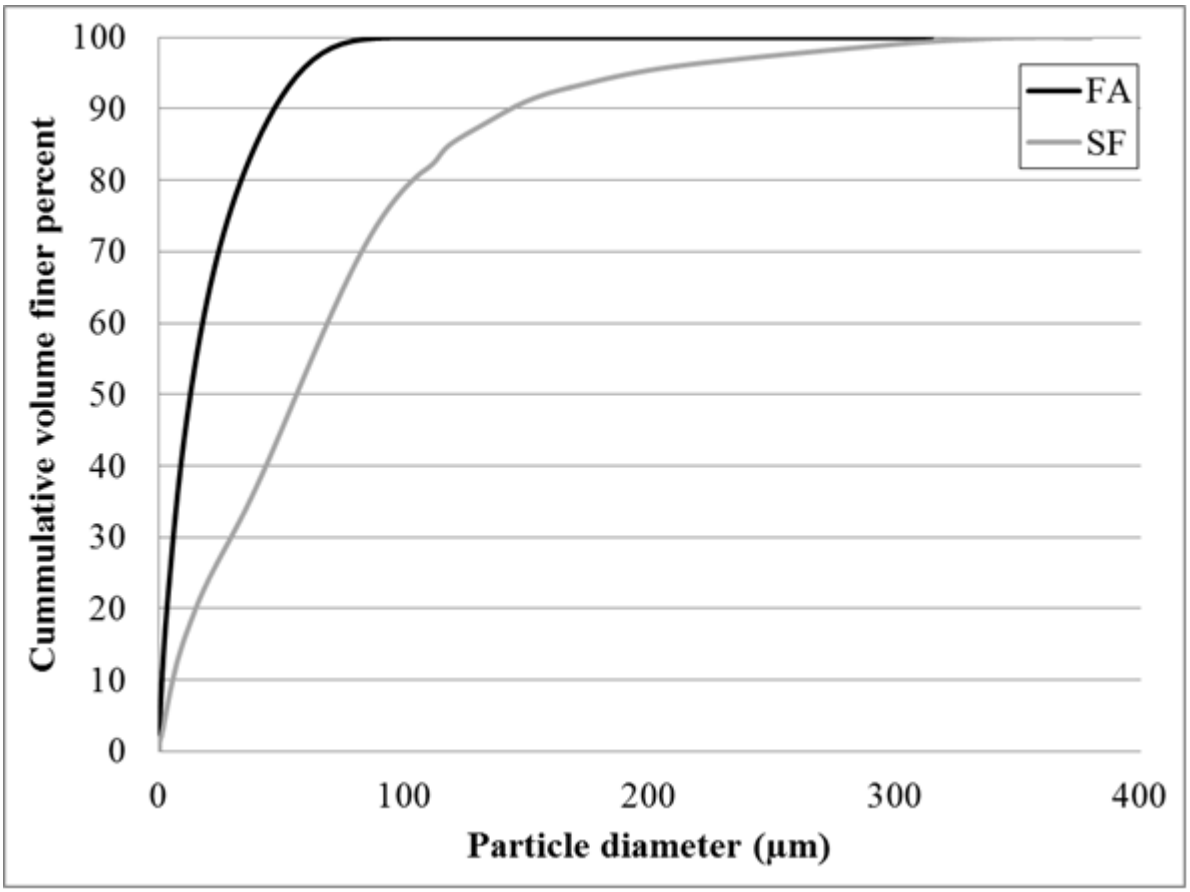

As can be seen in Figure 1, FA presented the finest particle size distribution, with 88 % of particles less than 45 µm. SF showed a coarser distribution than FA, with 80 % of particles lower than 100 µm.

Two activating solutions were used in this work. The first solution was a mixture of potassium silicate solution (SiO_2 23 w/w % and K_2O 14.9 w/w %) (Industrias Químicas del Ebro, Spain) and sufficient potassium hydroxide to increase the K_2O/SiO_2 molar ratio up to 1.45 (pH = 13.5). The second solution was KOH 8M (pH = 14).

2.2 Geopolymeric foam preparation

Geopolymeric foams were manufactured in a laboratory mixer working at 500 rpm. Fly ash was mixed with an activating solution until a thixotropic paste was obtained (mixing time was 4 minutes). After that, silica fume was added to the geopolymer paste. A reduction in thixotropy and workability of the geopolymers was observed as SF was mixed with the geopolymer paste, so extra water was necessary to improve both characteristics. The pastes obtained were poured into cylindrical plastic moulds (30 mm-diameter and 40 mm-height). Two setting temperatures were studied: 40 ºC and 70 ºC (in the first 24 hours). After setting, samples were demoulded and cured at room temperature (average temperature: 20 ºC; average relative humidity: 45 %) for a further 27 days. Compositions of geopolymeric foams are detailed in Table 2. The samples were cut after 28 days in order to obtain the same sample thickness (40 mm) in the different tests.

Table 2. Composition of geopolymeric foam

Geopolymer foam	Solid phase (wt%)		Activating solution (g)/Fly ash (g)	Water (g)/Solid phase (g)	Setting temperature (ºC)
	FA	SF			
FA100SF0-KSil-40ºC	100	0	0,74	0	40
FA80SF20-KSil-40ºC	80	20	0,74	0,1	40
FA60SF40-KSil-40ºC	60	40	0,74	0,225	40
FA80SF20-KSil-70ºC	80	20	0,74	10	70
FA80SF20-KOH-40ºC	80	20	0,71	0	40

As can be seen in Table 2, three parameters have been studied: FA-SF proportion (100-0, 80-20, 60-40), activating solution (potassium silicate (KSil) vs potassium hydroxide (KOH)), and setting temperature (40 vs 70 ºC). As the silica fume content increased in the mixture, the water/solid ratio also increased. This phenomenon suggests that SF may demonstrate inert material behaviour in the geopolymerization reaction. As the addition of SF produced a foam material, final products obtained from samples FA80SF20 and FA60SF40 were also named geopolymeric foams. However, the final product of the sample FA100SF0 was a geopolymeric paste.

2.3. Methods

2.3.1. Volume expansion and setting time

The geopolymerization reaction kinetic was studied analysing the setting time. The setting time was determined using a Vicat needle (EN 196-3) [34]. The initial setting time is the time elapsed between the initial instant and the time in which the distance from the needle to the bottom base of the cylinder is 6±3 mm. The final setting time is the time between the initial instant and the time in which the needle shows no visible signal on the upper base of the cylinder. The pore generation reaction kinetic was determined by measuring the expansion volume (EV) of material during setting (mm). EV is the ratio between the foam volume at instant t, V(t), and the initial volume of introduced paste, V(0). For this test, geopolymer samples were moulded in 35 mm-diameter and 80 mm-high cyclindrical plastic molds no more than half-full. Three specimens of each geopolymer mixtures were used to determine the volume expansion and setting time.

2.3.2. XRD analysis

Geopolymer samples were studied by means of X-ray powder diffraction (XRD) to evaluate their mineralogical composition. A D8 Advance A25 (BRUKER) (40 kV and 30 mA) instrument was used and phase identification was carried out using DIFFRAC.EVA software (BRUKER).

2.3.3. Physical and mechanical properties

Density (ρ) of the geopolymers was measured in accordance with the EN 1936 standard method [35]. Open void ratio (open porosity) was also determined because it is strongly related to the acoustic behaviour of the products. The method of vacuum water saturation was followed in the determination of open porosity (OP %) [35].

Compressive strength of geopolymer samples was determined in accordance with EN 196-1 [36], using a Tinius Olsen-TO317EDG machine. Four specimens of each geopolymer (paste or foam) were used to determine the compressive strength, density and open porosity.

2.3.4. Acoustic properties

In order to evaluate the acoustic properties of the geopolymeric samples, sound absorption was determined using a Kundt tube, according to EN ISO 10534-2 [37]. An ACUPRO system, implemented by "Spectronics Inc.", with two microphones and a SAMSON signal amplifier, was used. Three specimens of each geopolymer have been tested. The thickness of all the tested specimens was 40 mm. The Noise Reduction Coefficient (NRC) was determined by calculating the arithmetic mean of the absorption coefficients at 250 Hz, 500 Hz, 1000 Hz and 2000 Hz.

3. RESULTS

3.1. Expansion volume and setting evolution with time

Figures 2, 3 and 4 show the setting curves (penetration of Vicat needle (mm) in the cylinder versus time) (Set) and the expansion volume curves (expansion volume data (natural logarithm) (EV) versus time), taking into account the three parameters studied: FA-SF proportion (100-0, 80-20, 60-40) in Figure 2, activating solution (potassium silicate vs potassium hydroxide) in Figure 3 and setting temperature (40 vs 70 ºC) in Figure 4. Standard deviations are also represented as error bars.

Figure 2. Expansion volume and setting curves for different FA-SF proportions

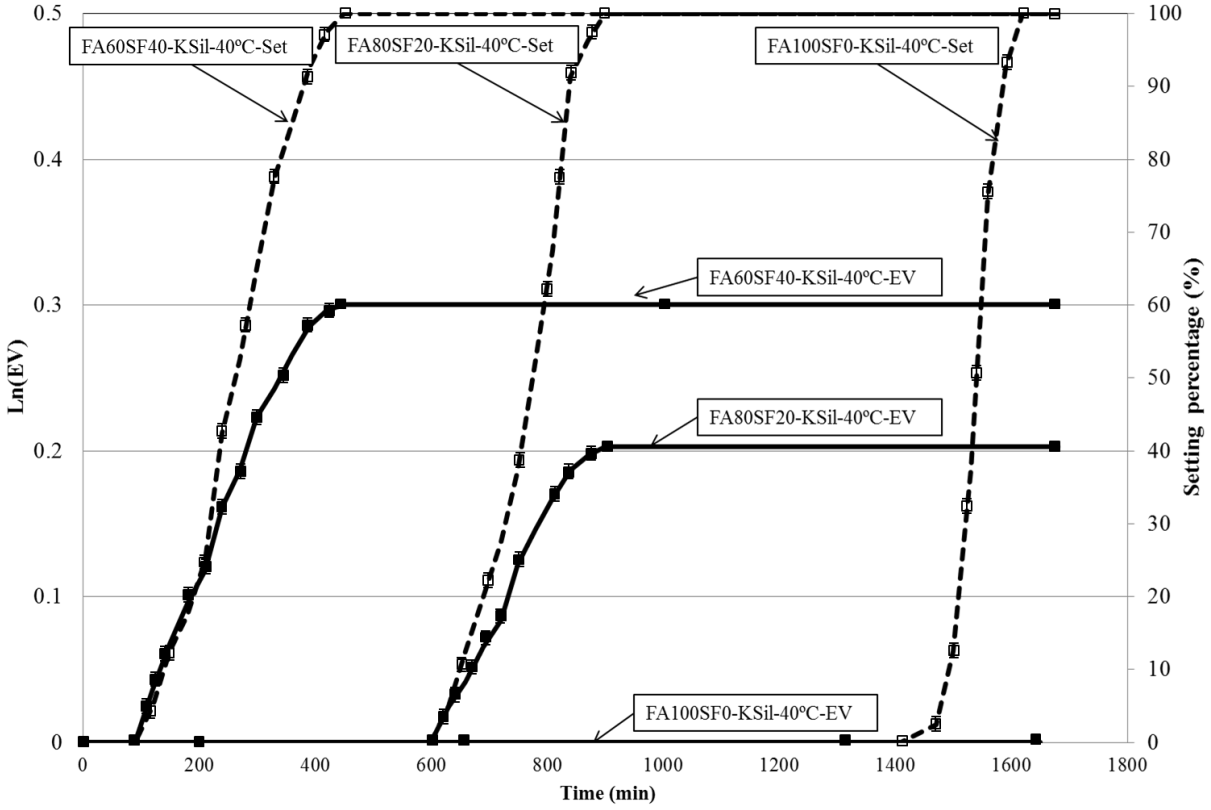

Figure 2 shows that the substitution of FA with SF produced a reduction in the initial setting time (from 1410 min for geopolymer paste without silica fume (FA100SF0) to 120 min for geopolymer foam with 40 %wt of silica fume (FA60SF40)) and final setting time (from 1620 min without silica fume to 450 min with 40 % wt of silica fume). Figure 2 also shows an increment in material expansion volume as silica fume was added to the mixture due to generation of gas produced by the use of SF (as SF content was null, EV was null).

Figure 3. Volume expansion and setting curves for different activating solutions (potassium silicate vs potassium hydroxide)

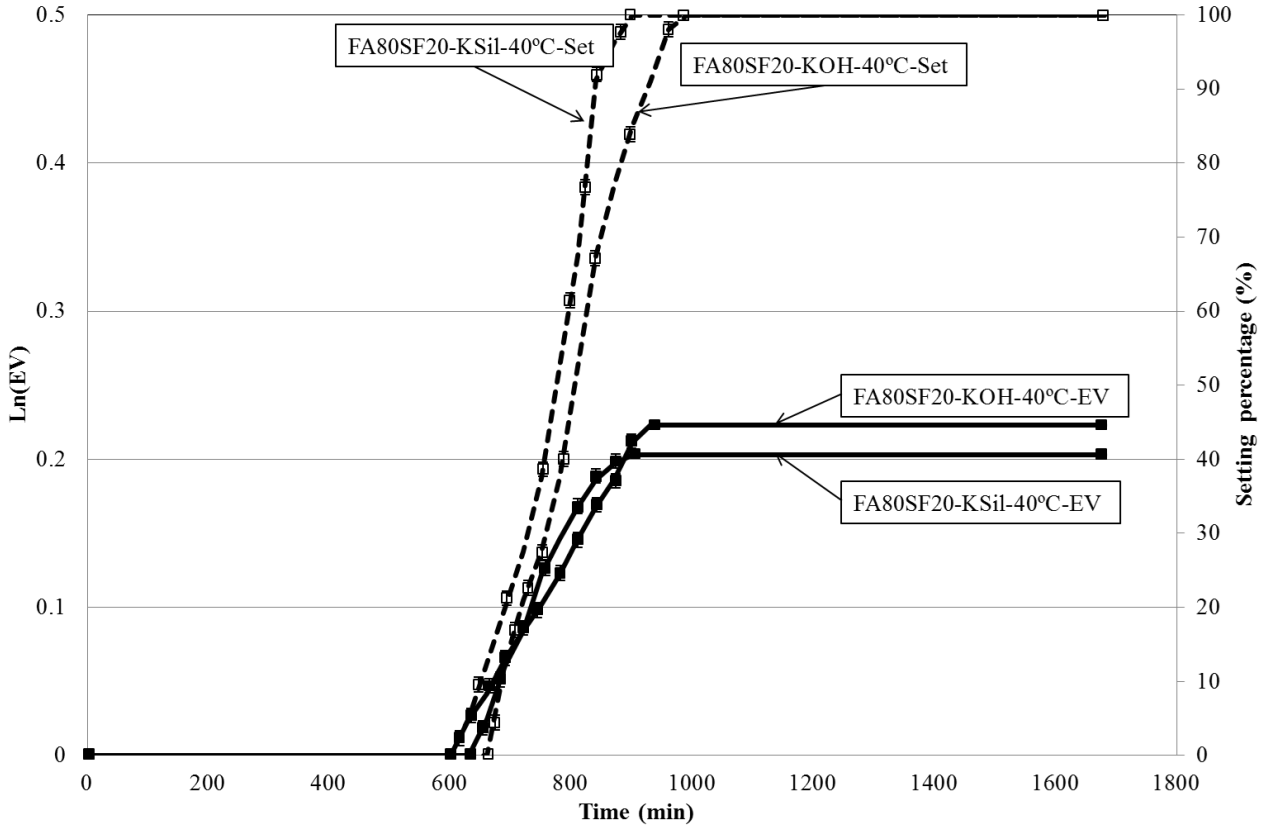

As can be seen in Figure 3, the change of activating solution did not bring about important variations in setting time and material expansion volume results. A slight reduction in the setting time in geopolymer foam activated with potassium silicate in comparison with the activation with potassium hydroxide was observed. A slight increment in expansion volume as geopolymer foam was activated with potassium hydroxide can also be observed.

Figure 4. Volume expansion and setting curves for different setting temperatures (40 vs 70 ºC)

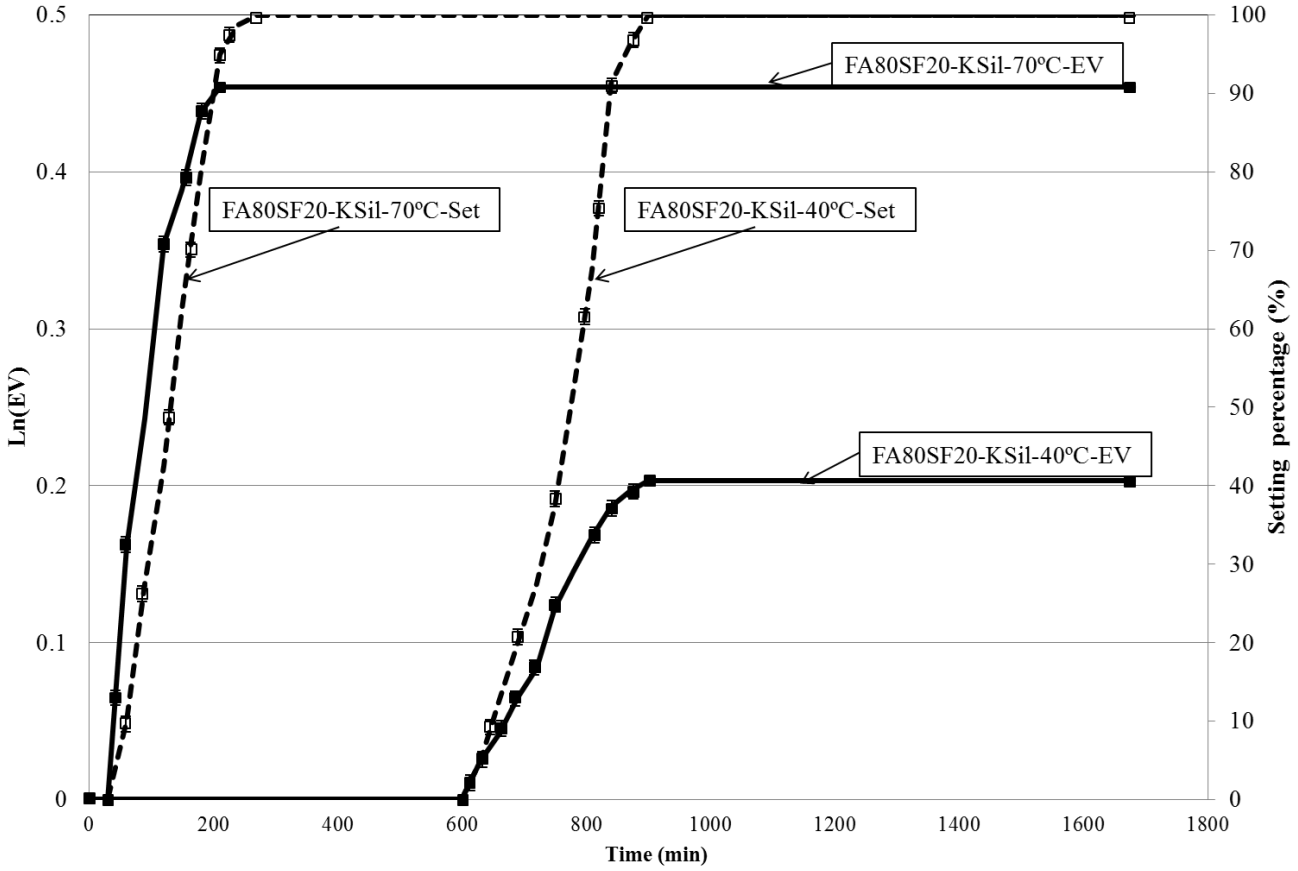

Figure 4 shows a reduction in the setting time as the geopolymer was set at 70 ºC (final setting time was 240 min) instead of 40 ºC (final setting time was 870 min). An increase in material expansion with the temperature (more than 100 %) was also observed.

3.2. XRD analysis

XRD patterns of FA, SF, geopolymer FA100SF0-KSil and geopolymer foam FA60SF40-KSil set at 40 ºC are detailed in Figure 5.

Figure 5. XRD patterns of FA, SF, geopolymer FA100SF0-KSil and geopolymer foam FA60SF40-KSil set at 40 ºC

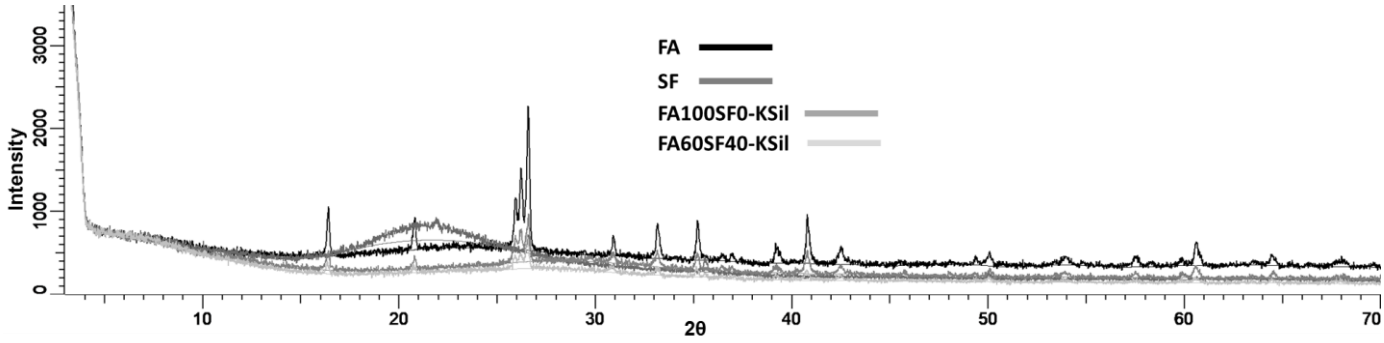

SF pattern was characteristic of an amorphous material, with a broad peak in the 2θ range 15-30. FA showed a slight broad peak between 15-38 values of 2θ, so FA could be considered a type of amorphous degree material. Some crystalline peaks were also detected in FA, mainly quartz and mullite. The geopolymer FA100SF0-KSil and the geopolymer foam FA60SF40-KSil exhibited very similar patterns analogous to the the FA pattern. They showed a slight shift of the broad reflection regarding the FA pattern, with lower intensity peaks of quartz and mullite than the FA.

3.3. Physical and mechanical properties

3.3.1. Open porosity and apparent density

Open porosity and density of geopolymer samples at 28 days of curing are detailed in Table 3. Standard deviations are also specified for open porosities and densities.

Table 3. Open porosity and density

Geopolymer foam	Open porosity (%)	Density (g/cm^3)
FA100SF0-KSil-40ºC	11.5±1.2	1.4±0.1
FA80SF20-KSil-40ºC	18.1±1.8	1.17±0.1
FA60SF40-KSil-40ºC	28.9±2.5	1.07±0.1
FA80SF20-KSil-70ºC	36.2±3.2	0.97±0.1
FA80SF20-KOH-40ºC	20.1±2.1	1.12±0.1

Open porosity increased and density decreased as silica fume proportion in the mixture was increased and as setting temperature was changed from 40 ºC (open porosity of 18.1%) to 70 ºC

(open porosity of 36.2%). Open porosities displayed a slight variation as the activating solution was modified. The geopolymer foam activated with potassium silicate showed a porosity value of 18.1%. The value was 20.1% as the geopolymer foam was prepared with potassium hydroxide.

3.3.2. Compressive strength

Figures 6 shows the effect of FA-SF proportion on the compressive strength values determined at 1 day and 28 days of curing. Standard deviations are represented as error bars.

Figure 6. Compressive strength. FA-SF proportion

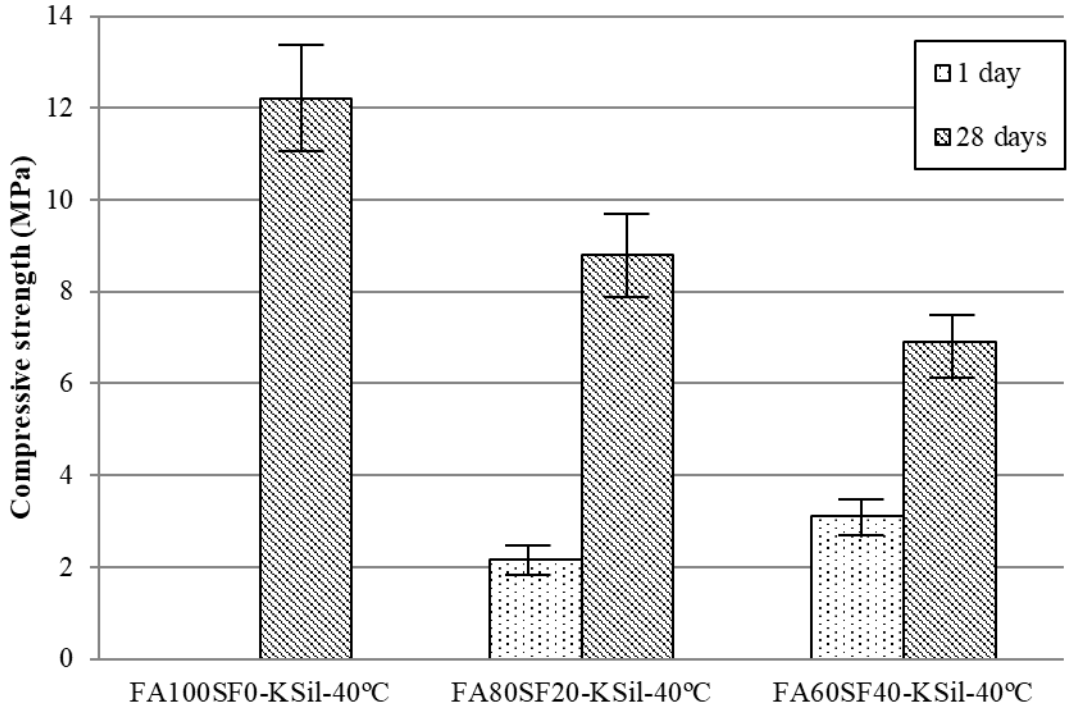

Two different behaviors depending on the curing time have been observed: a positive effect of silica fume in compressive strength at early stages (1 day) of curing and a negative effect in the final stages (28 days). As can be seen, there was no compressive strength data of the geopolymer paste (FA100SF0-KSil) because this material did not set at 1 day.

Figure 7 represents the compressive strength results at 1 day and 28 days of curing for geopolymer foams activated with silicate and hydroxide. Standard deviations are detailed as error bars.

Figure 7. Compressive strength. Activating solution (potassium silicate vs potassium hydroxide)

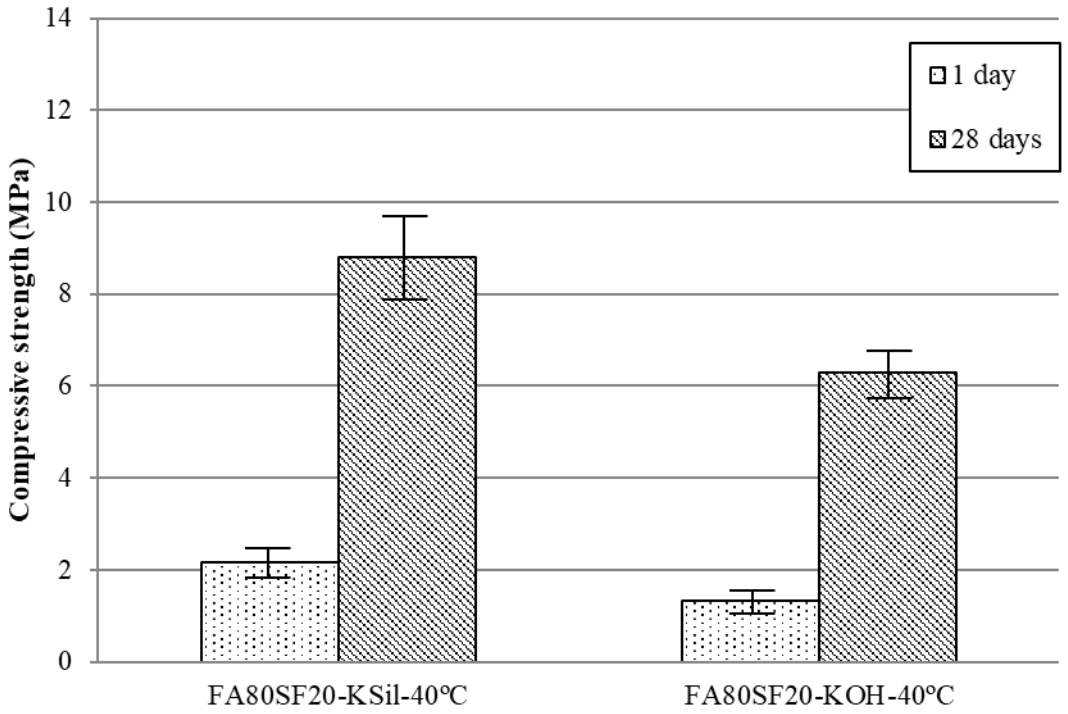

The setting time was slightly higher in geopolymer activated with potassium hydroxide than with potassium silicate, so the compressive strength at 1 day of hydroxide activated geopolymer foam was slightly lower than silicate activated geopolymer foam. The same tendency was observed at 28 days of curing; geopolymer foam activated with potassium silicate was stronger than that activated with potassium hydroxide.

The effect of setting temperature on compressive strength of the geopolymer foams is displayed in Figure 8. Standard deviations are specified as error bars.

Figure 8. Compressive strength. Setting temperature (40 vs 70 ºC)

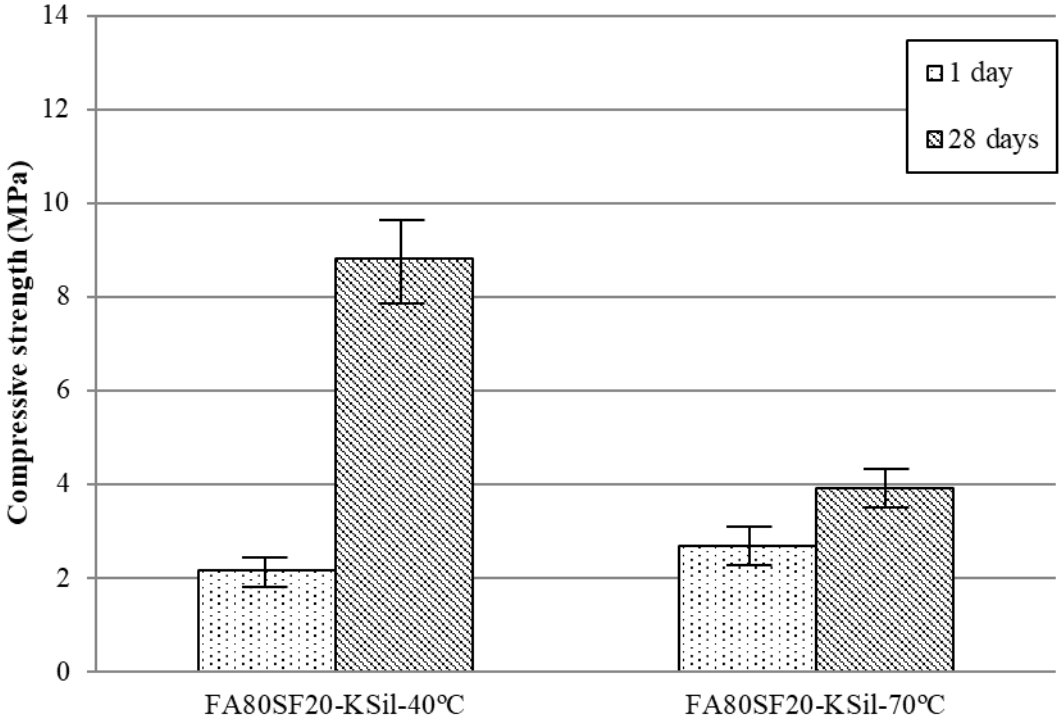

As can be seen, the setting at 70 ºC had a positive effect on the compressive strength at early stages but the effect is negative at 28 days of curing.

3.4. Acoustic properties

Figures 9, 10 and 11 show the sound absorption coefficient curves, taking into account the three parameters studied. The sound absorption coefficient is represented in 1/3 octave band of the frequencies between 100-5000 Hz. Standard deviations are represented as error bars.

Figure 9. Sound absorption coefficient. FA-SF proportion

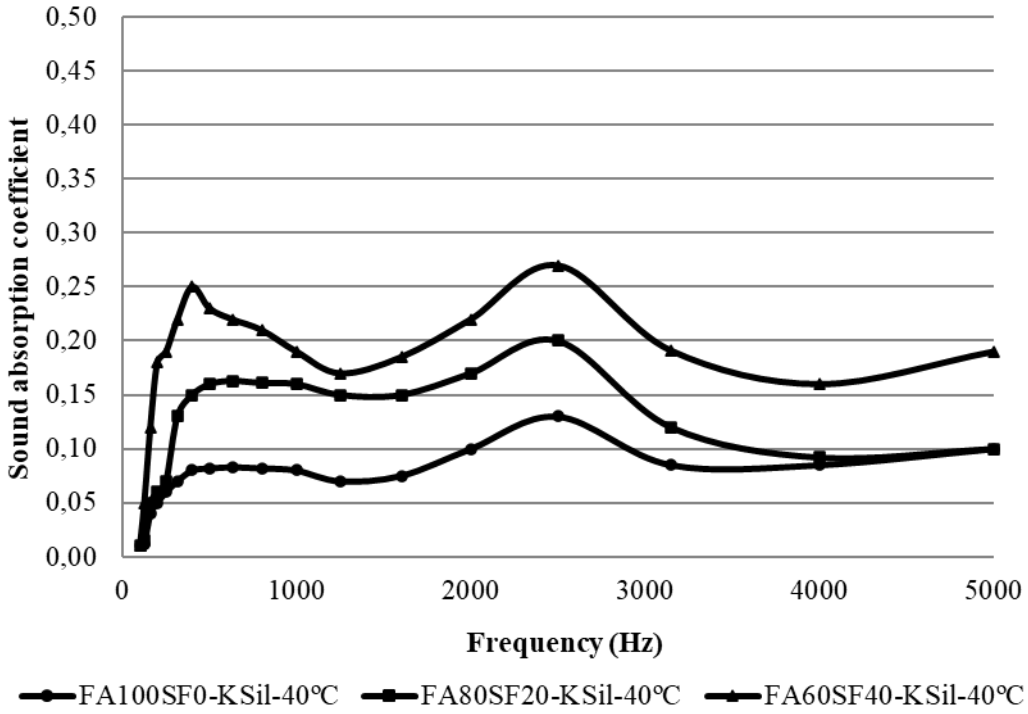

Figure 9 shows that the three curves had similar shapes (with two peaks at 400 and 2500 Hz, respectively). As can be seen, the greater the silica fume proportions in the mixture, the higher the breadth curve, which could be correlated with the highest open porosity.

Figure 10. Sound absorption coefficient. Activating solution (potassium silicate vs potassium hydroxide)

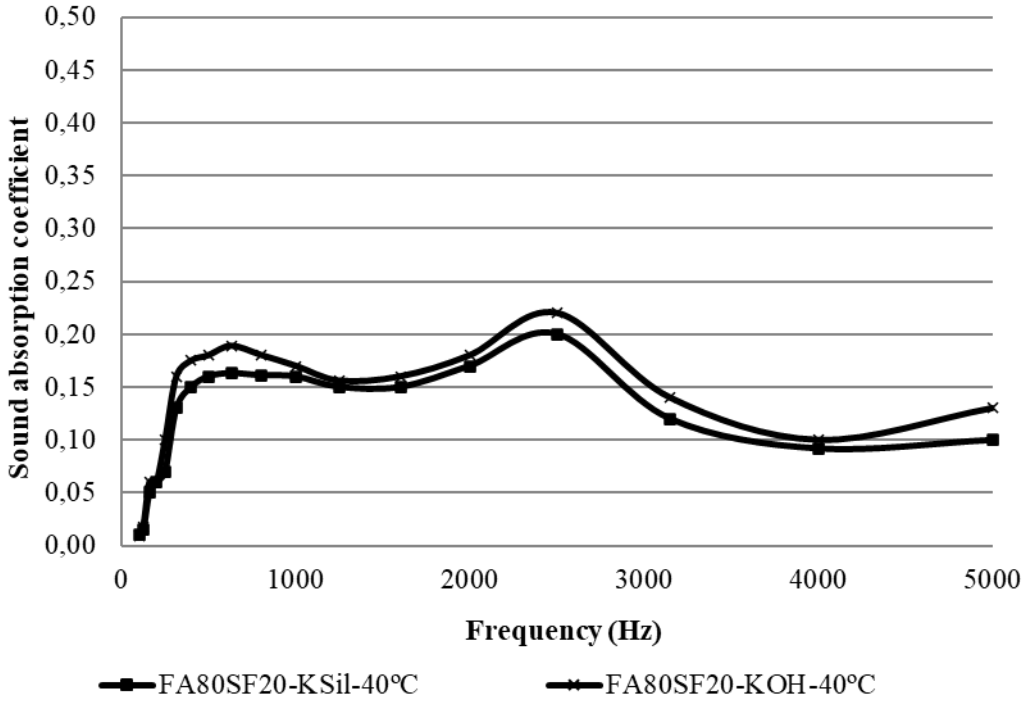

As can be seen in Figure 10, both curves were extremely similar (the curve of geopolymer foam activated with hydroxide was marginally above the curve of geopolymer foam activated with silicate). Both geopolymer foams had a similar open porosity (slightly higher open porosity was observed in the geopolymer foam activated with hydroxide), which may explain the similarity between the curves.

Figure 11. Sound absorption coefficient. Setting temperature (40 vs 70 ºC)

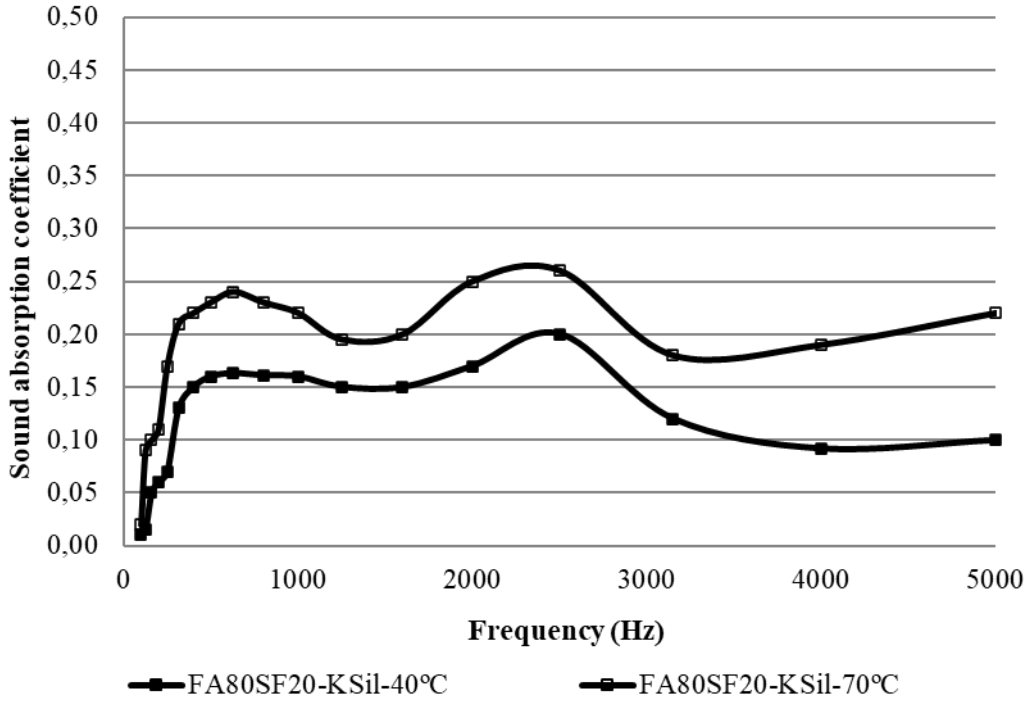

Figure 11 shows that both curves had a similar shape. Two peaks at 400 and 2500 Hz were also observed. The highest values of the sound absorption coefficient were observed in the geopolymer foam set at 70 ºC since this material presented the greatest open porosity.

Noise Reduction Coefficient (NRC) for all geopolymers is detailed in Table 4. This coefficient is a numerical descriptor of the sound absorption, which is very useful to make comparisons. Standard deviations are also detailed. Analysing Table 4 and Table 3 we can see that the NRC increased as porosity increased.

Table 4. NRC of geopolymer foams

Geopolymer foam	NRC
FA100SF0-KSil-40ºC	0.08±0.01
FA80SF20-KSil-40ºC	0.14±0.01
FA60SF40-KSil-40ºC	0.21±0.02
FA80SF20-KSil-70ºC	0.23±0.02
FA80SF20-KOH-40ºC	0.16±0.01

4. DISCUSSION

4.1. Volume expansion and setting time

Two reactions take place during the geopolymer foam manufacture: the geopolymerization reaction and the pore generation reaction. The geopolymerization reaction occurs when the fly ash reacts with the activating solution, producing an alkali aluminosilicate hydrated gel. The gel obtained in the current work was mainly based on potassium (potassium aluminate silicate hydrated gel) since the activating solution contains potassium as alkali cation [38]. The use of different types of anions (silicate or hydroxides) also affects the final chemical composition of the gel (Si/Al ratios are higher in gels after activation with silicate than with hydroxide) [38, 39]. The pore generation is due to the H_2(g) released during the water reduction and silicon (from silica fume) oxidation, producing $Si(OH)_4$. The reaction is promoted in basic medium [24] according to:

$$4H_2O + Si \rightarrow 2H_2\,(g) + Si(OH)_4 \qquad \text{(eq 1)}$$

As can be seen in Figures 2, 3 and 4, setting curves exhibited three clearly differentiated stages. The first stage corresponded to the plastic period of the geopolymer, which goes from the time in which needle penetrates completely to the start of setting. The second stage matched with the setting period of the geopolymer, which is between initial and final setting time (needle shows resistance to penetration). The final stage constituted the hardening period.

Expansion volume curves also showed three stages. The first stage began with a period of latency during which the expansion volume was null, named latency time [30]. The second stage of the curve exhibited an increase of expansion volume (EV) with the time caused by the generation of gas, which follows a linear regime [30]. The last showed a final expansion volume constant through time.

The replacement of fly ash with silica fume produced a reduction in the initial and final setting time of the geopolymer, that is, the geopolymer paste FA100SF0 set more slowly than the geopolymer foam FA80SF20 and the geopolymer foam FA80SF20 more slowly than FA60SF40. This behavior

is similar in silica fume blended cement pastes [40] or in silica fume blended metakaolin geopolymers [24] where an increment in silica fume accelerated the setting and hardening process. An increment in material expansion volume as silica fume was added to the mixture was also observed. This is due to the generation of gas produced by the use of SF (according to equation 1). In addition, the latency period matched the plastic period and the setting time coincided with the period in which gas was generating. As gas is generated, the hydrogen bubbles try to escape from the material. When the geopolymer is still fluid in the plastic period (setting has not yet taken place), the gas bubbles generated can leave the geopolymer. However, while the geopolymer is setting and the material is hardening, the gas becomes trapped in the structure, expanding the geopolymeric matrix and increasing the expansion volume.

The type of activating solution did not significantly affect the setting time or the expansion volume. A slight reduction in the setting time of geopolymer foam activated with potassium silicate compared with that activated with potassium hydroxide was observed. Some authors [39] noted that geopolymers activated with soluble silicate showed higher reaction rates than those activated with hydroxide. Furthermore, previous work of the authors [41], where the activation with hydroxide versus silicate was studied, concluded that systems activated with hydroxide (KOH 8M) presented (fewer) lower degrees of reaction, at the same time, than systems activated with silicates (potassium silicate), which could provide evidence of the high rate of reaction with silicates. Furthermore, pH of the activating solution must be also considered. Some authors [42] revealed that high concentration solutions presented a coagulation of silica, reducing the dissolution of Si^{4+} and Al^{3+} from the raw material. In the current work, pH of potassium hydroxide solution was >14 and pH of potassium silicate solution was 13.5. Therefore, the increase in setting time using KOH 8M could be the result of some silica coagulation, which may result in some setting delay.

Material expansion volume was slightly higher in geopolymer activated with potassium hydroxide, possibly due to the different solution pH (pH>14 in the potassium hydroxide solution and pH = 13.5

293 in the potassium silicate solution). As previously mentioned, the pore generation reaction occurs in
294 basic medium, so the addition of a more basic solution could have a positive effect on this reaction.
295 The effect of temperature is also displayed, showing a reduction in setting time and an increment in
296 material expansion as geopolymer foam samples set at 70 ºC instead of 40 ºC. On one hand, it is
297 well known that temperature is a geopolymerization reaction accelerator [39]. On the other hand,
298 the reaction of equation 1 is enhanced by the temperature [43]. Henon et al. [30] have proposed that
299 the final expansion of metakaolin based geopolymer with silica fume followed an Arrhenius law
300 with the temperature, obtaining a value of activation energy of 11.9 kJ/mol. The activating energy
301 of geopolymer foam FA80SF20-KSil in the current work was also calculated according to the
302 methodology of Henon's work and the value was 27.9 kJ/mol. This value was similar to that
303 obtained in a study carried out by Provis [44] (33 kJ/mol) where metakaolin was used as
304 geopolymeric raw material.
305 4.2. XRD analysis
306 XRD results show the changes which took place in the SF and the FA after the geopolymerization
307 reaction. As previously mentioned, FA displayed a slight broad reflection in the 2θ range 15-38
308 with crystalline peaks of quartz and mullite. The geopolymer paste FA100SF0-KSil showed a shift
309 of the broad peak in the 2θ range 22-38 regarding the FA pattern, which provides evidence of the
310 dissolution of SiO_4 and AlO_4 species during the geopolymerization reaction [24]. In addition, the
311 crystalline peaks in the geopolymer (quartz and mullite) were in the same 2θ position as the FA
312 pattern but with lower intensity, which was indicative of alteration of the crystal structure [23]. SF
313 pattern was characteristic of an amorphous material, with a broad peak, which was not found in the
314 geopolymer foam FA60SF40-KSil pattern. The geopolymer foam pattern was rather similar to the
315 geopolymer paste and the FA patterns, with a slight shift of the broad peak in the 2θ position and
316 with the crystalline peaks (quartz and mullite) in the same place but with lower intensity.
317 Comparing the XRD patterns of the geopolymer paste and the geopolymer foam we can see that the

318 silica fume addition did not produce significant differences in amorphous and crystalline phases,
319 except a slight difference in the intensity of the peaks. Amorphous content of both materials were
320 calculated using DIFRACT.EVA software to support these results. FA100SF0 and FA60SF40
321 showed values of 51.6 % and 53.8 %, respectively.
322 4.3. Physical and mechanical properties
323 Table 3 and Figures 2, 3 and 4 provide evidence of the direct relationship between open porosity
324 and expansion volume of the material. The material expansion test (Figure 2) shows higher foam
325 development of the geopolymer as the proportion of silica fume increased, which allows us to view
326 the positive effect of silica fume proportion in pore generation, and consequently, in the open
327 porosity. The same behavior was displayed as the activating solution effect was analyzed.
328 Geopolymer foam activated with hydroxide (Figure 3) showed a slightly higher expansion volume
329 than that activated with potassium silicate, so the amount of generated pore was slightly greater, as
330 was the open porosity. The values of open porosity depend greatly on the setting temperature,
331 producing a high increment in open porosity as the temperature increased from 40 to 70 ºC due to
332 the increment in the expansion volume (Figure 4). Photographs of different geopolymer foams are
333 detailed in Figure 12. Analyzing the pore size in the right photograph, it can be observed that pore
334 sizes were in the range 1-3 mm, which are the most appropriate pore sizes for noise absorbing
335 materials [45].
336 **Figure 12. View of the some of the geopolymer foam (A. FA100SF0-40ºC; B. FA60SF40-40ºC;**
337 **C. FA80SF20-40ºC; D. FA80SF20-70ºC) after 28 days of curing**

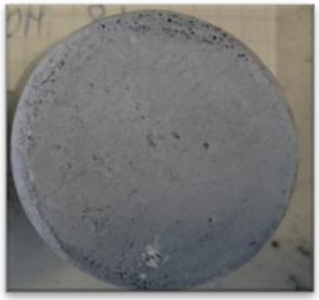

A. FA100SF0-40 ºC

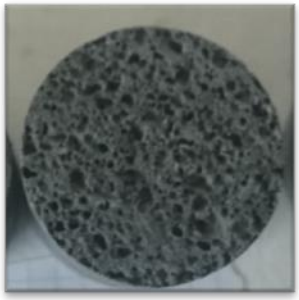

B. FA60SF40-40 ºC

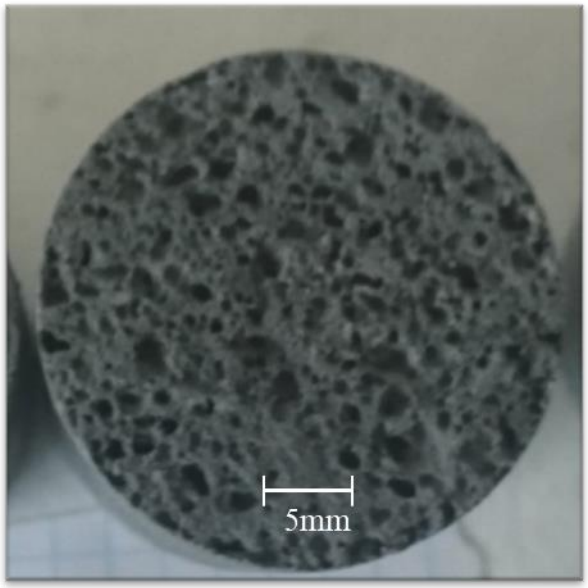

B. FA60SF40-40 ºC

C. FA80SF20-40 ºC

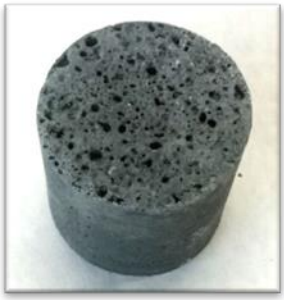

D. FA80SF20-70 ºC

The effect of silica fume content, activating solution and setting temperature on compressive strength depend on the curing time in which the test was carried out: early stages (1 day) or final stages (28 days). It seems that compressive strength at early stages was controlled by the setting rate. Therefore, variables that produce quick setting times such as using a high content of silica fume (up to 40%), to set at 70 ºC and to activate with potassium silicate, can improve the compressive strength at 1 day of curing. However, the compressive strength at final stages was controlled by the open porosity values. The parameters that reduced the open porosity (no use of silica fume, to set at 40 ºC and to activate with potassium silicate) also produced an enhancement of the compressive strength at 28 days of curing. It is well known that an increase in voids or pores in any material (while the rest of the parameters remain unchanged) always causes a reduction in the compressive strength since the volume/resistant mass ratio is lower [46], so the poorest mechanical properties were observed in the most porous geopolymer foams.

4.4. Acoustic properties

Taking into account that sound absorption in a porous material is related to the energy loss through friction with the wall of the holes, higher porous structures showed higher sound absorbing properties [12]. Therefore, to increase the silica fume proportion and to increase the setting temperature from 40 to 70 ºC produced a positive effect on sound absorption. In addition, these geopolymer foams exhibited sound absorption coefficients similar to or better than commercial porous concrete [46] and other sound absorption materials containing wastes, such as bottom ashes [46] or ceramic wastes [47].

5. CONCLUSIONS

The main aim of this experimental study was to develop geopolymeric foams using fly ash and silica fume. The foam products presented porous material characteristics with relatively good noise absorption properties. Three parameters have been studied: silica fume content, activating solution and setting temperature. Five properties have been evaluated: setting time, expansion volume, open porosity, compressive strength (at early and final stages) and sound absorption, all of which are closely linked.

The substitution of fly ash with silica fume and the set at 70 ºC reduced the initial and final setting time and increased material expansion. The first observed effect was an increment in the open porosity of the geopolymer foam. Taking into account that the sound absorption in a porous material was related to the energy loss through friction with the walls of the holes, less porous structures showed lower sound absorbing properties. Therefore, geopolymer foam prepared with the highest amount of silica fume and set at 70 ºC showed the greatest noise reduction coefficient. The effect of the three parameters on compressive strength depends on the curing time. The behaviour of the materials at early and final stages of curing is not the same since the compressive strength values at early stages (1 day) were controlled by the setting rate. However, the compressive strength values at 28 days were directly related to the open porosity values.

It seems that to replace one activating solution for another did not produce significant differences. A slight reduction in setting time using silicate, and a slight increment in open porosity (expansion volume) using hydroxide was observed, possibly due to the variations in the pH values of solutions and the different degrees of reaction reached by the different material products obtained.

Compliance with Ethical Standards:

Authors declare that they have no conflicts of interest.

Acknowledgements:

Authors would like acknowledge the help received by CITIUS (General Research Services) from University of Seville, especially the XRD laboratory.

References

[1] Zhang L, Zhang F, Liu M, Hu X. Novel sustainable geopolymer based syntactic foams: An eco-friendly alternative to polymer based syntactic foams. Chem. Eng. J. 313 (2017) 74-82. DOI: 10.1016/j.cej.2016.12.046.

[2] Palomo A, Krivenko P, Garcia-Lodeiro I, Kavalerova E, Maltseva O, Fernández-Jiménez A. A review on alkaline activation: new analytical perspectives. Mater. Construcc. 64(315) (2014) e022. https://doi.org/10.3989/mc.2014.00314.

[3] Yunsheng Z, Wei S, Qianli C, Lin C. Synthesis and heavy metal immobilization behaviours of slag based geopolymer. J. Hazard. Mater. 143(1–2) (2007) 206–213. DOI: 10.1016/j.jhazmat.2006.09.033

[4] Luna-Galiano Y, Fernandez Pereira C, Vale J. Stabilization/solidification of a municipal solid waste incineration residue using fly ash-based geopolymers. J. Hazard. Mater. 185(1) (2011) 373–381. DOI: 10.1016/j.jhazmat.2010.08.127

[5] Zhang J, Provis JL, Feng D, van Deventer JSJ. Geopolymers for immobilization of Cr(6+), Cd(2+), and Pb(2+). J. Hazard. Mater. 157(2–3) (2008) 587–598. DOI: 10.1016/j.jhazmat.2008. 01. 053

[6] Fernández Pereira C, Luna-Galiano Y, Querol X, Antenucci D., Vale J. Waste stabilization/solidification of an electric arc furnace dust using fly ash-based geopolymers. Fuel. 88(7) (2009) 1185-1193. DOI: 10.1016/j.fuel.2008.01.021.

[7] Zhang HY, Kodur V, Qi SL, Cao L, Wu B. Development of metakaolin–fly ash based geopolymers for fire resistance applications. Constr. Build. Mater. 55 (2014) 38-45. DOI: 10.1016/j.conbuildmat.2014.01.040

[8] Zhang HY, Kodur V, Qi SL, Wu B, Cao L, Fan Wang. Thermal behavior and mechanical properties of geopolymer mortar after exposure to elevated temperatures. Constr. Build. Mater. 109 (2016) 17-24. DOI: 10.1016/j.conbuildmat.2016.01.043

[9] Luna-Galiano Y, Cornejo A, Leiva C, Vilches LF, Fernández-Pereira C. Properties of fly ash and metakaolín based geopolymer panels under fire resistance tests. Mater. Construcc. 65(319) (2015) e059. http://dx.doi.org/10.3989/mc.2015.06114.

[10] Luna-Galiano Y, Leiva C, Arenas C, Arroyo F, Vilches LF, Fernández Pereira C, Villegas R. Behaviour of Fly Ash-Based Geopolymer Panels Under Fire. Waste. Biomass. Valor. 8(7) (2017) 2485-2494. DOI: 10.1007/s12649-016-9803-y

[11] Luna-Galiano Y, Arenas C, Cornejo A, Leiva C, Vilches LF, Fernández-Pereira C. Recycling by-products from coal-fired power stations into different construction materials. Int. J. Energ. Environ. Eng. 5 (2014) 387–397. DOI: 10.1007/s40095-014-0120-6

[12] Arenas C, Luna-Galiano Y, Leiva C, Vilches LF, Arroyo F, Villegas R, Fernández-Pereira C. Development of a fly ash-based geopolymeric concrete with construction and demolition wastes as aggregates in acoustic barriers. Constr. Build. Mater. 134 (2017) 433–442. https://doi.org/10.1016 /j.conbuildmat.2016.12.119

427 [13] Zhang Z, Provis JL, Reid A, Wang A. Mechanical, thermal insulation, thermal resistance and
428 acoustic absorption properties of geopolymer foam concrete. Cem. Concr. Com. 62 (2015) 97-105.
429 https://doi.org/10.1016/j.cemconcomp.2015.03.013
430 [14] MacKenzie KJD. Innovative applications of inorganic polymers (geopolymers). Handbook of
431 Alkali-Activated Cements, Mortars and Concretes. Pacheco-Torgal F, Labrincha J, Leonelli C,
432 Palomo A and Chindaprasirt P (eds) (2015) 777-805.
433 [15] Duxson P, Provis JL, Lukey GC, Van Deventer JSJ. The role of inorganic polymer technology
434 in the development of `green concrete´. Cem. Concr. Res. 37 (2007) 1590-1597. DOI: 10.1016/
435 j.cemconres.2007.08.018
436 [16] Van Jaarsveld JGS, Van Deventer JSJ, Lorenzen L. The potencial use of geopolymeric
437 materials to immobilise toxic metals: Part I. Theory and applications. Miner. Eng. 10(7) (1997) 659-
438 669. DOI: 10.1016/S0892-6875(98)00121-6
439 [17] Bakharev T. Resistance of geopolymer materials to acid attack. Cem. Concr. Res. 35(4) (2005)
440 658-670. DOI: 10.1016/j.cemconres.2004.06.005
441 [18] Davidovits J. Properties of geopolymers cements. In: Proceedings of First International
442 Conference on Alkaline Cements and Concretes. Krivenko P (eds), Kiev, Ukraine (1994) 131-149.
443 [19] Zhang Z, Provis JL, Reid A, Wang H. Geopolymer foam concrete: An emerging material for
444 sustainable construction. Constr. Build. Mater. 56 (2014) 113-127. DOI: 10.1016/j.conbuildmat.
445 2014.01.081
446 [20] Cilla MS, Morellia MR, Colombob P. Open cell geopolymer foams by a novel
447 saponification/peroxide/gelcasting combined route. J. Eur. Ceram. Soc. 34(12) (2014) 3133–3137.
448 DOI: 10.1016/j.jeurceramsoc.2014.04.001
449 [21] Arellano Aguilar R, Burciaga Díaz O, Escalante García JI. Lightweight concretes of activated
450 metakaolin-fly ash binders, with blast furnace slag aggregates. Constr. Build. Mater. 24(7) (2010)
451 1166-1175. DOI: 10.1016/j.conbuildmat.2009.12.024

452 [22] Hlaváček P, Šmilauer V, Škvára F, Kopecký L, Šulc R. Inorganic foams made from alkali-
453 activated fly ash: Mechanical, chemical and physical properties. J. Eur. Ceram. Soc. 35(2) (2015)
454 703-709. DOI: 10.1016/j.jeurceramsoc.2014.08.024
455 [23] Prud'homme E, Michaud P, Joussein E, Peyratout C, Smith A, Rossignol S. In situ inorganic
456 foams prepared from various clays at low temperature. Appl. Clay. Sci. 51(1–2) (2011) 15-22. DOI:
457 10.1016/j.clay.2010.10.016
458 [24] Prud'homme E, Michaud P, Joussein E, Peyratout C, Smith A, Arrii-Clacens S, Clacens JM,
459 Rossignol S. Silica fume as porogent agent in geo-materials at low temperature. J Eur Ceram. Soc.
460 30(7) (2010) 1641-1648. DOI: 10.1016/j.jeurceramsoc.2010.01.014
461 [25] Cilla MS, Colombo P, Morelli MR. Geopolymer foams by gelcasting. Ceram. Int. 40(4) (2014)
462 5723-5730. http://dx.doi.org/10.1016/j.ceramint.2013.11.011
463 [26] Masia G, Rickard WDA, Vickers L, Bignozzi MC, van Riessen A. A comparison between
464 different foaming methods for the synthesis of light weight geopolymers. Ceram. Int. 40(9) Part A
465 (2014) 13891–13902. DOI: 10.1016/j.ceramint.2014.05.108
466 [27] Neville AM. Properties of concrete, fifth eds, London, UK, Pearson (2011)
467 [28] ACI 116R, "Cement and Concrete Terminology," American Concrete Institute (2000).
468 [29] Papa E, Medria V, Kpogbemaboub D, Morinierec V, Laumonierc J, Vaccarid A, Rossignol S.
469 Porosity and insulating properties of silica-fume based foams. Energ. Buildings. 131 (2016) 223–
470 232. DOI: 10.1016/j.enbuild.2016.09.031
471 [30] Henon J, Alzina A, Absi J, Smith, DS, Rossignol S. Potassium geopolymer foams made with
472 silica fume pore forming agent for thermal insulation. J. Porous. Mater. 20(1) (2013) 37-46. DOI:
473 10.1007/s10934-012-9572-3
474 [31] ASTM C 618-05: 2005. Standard Specification for Coal Fly Ash and Raw or Calcined Natural
475 Pozzolan for Use in Concrete. ASTM International, USA.

476 [32] ASTM D3682-78: 1983. Test method for mayor and minor elements in coal and coke ash by
477 atomic absorption. ASTM International, USA.
478 [33] EN 1097-7:2009. Tests for mechanical and physical properties of aggregates - Part 7:
479 Determination of the particle density of filler - Pyknometer method.
480 [34] CEN (European Committee for Standardization) (2005) "EN 196-3: Methods of testing
481 cements: Part 3. Determination of setting times and soundness". Brussels, Belgium.
482 [35] EN 1936: 2006. Natural stone test methods - Determination of real density and apparent
483 density and total and open porosity.
484 [36] EN 196-1: 2006. Methods of testing cement - Part 1: Determination of strength. European
485 committee for standarisation. Brussels, Belgium.
486 [37] EN ISO 10534-2:1998. Acoustics determination of sound absorption coefficient and
487 impedance or admittance by the impedance tube. Part II: Transfer function method.
488 [38] Fernández-Jiménez A, Palomo A. Composition and microstructure of alkali activated fly ash
489 binder: Effect of the activator. Cem. Concr. Res. 35 (2005) 1984-1992. http://dx.doi.org/10.1016/
490 j.cemconres.2005.03.003.
491 [39] Palomo A, Grutzek, MW, Blanco MT. Alkali-activated fly ashes. A cement for the future.
492 Cem. Concr. Res. 29 (1999) 1323–1329. DOI: 10.1016/S0008-8846(98)00243-9
493 [40] Zhang W, Zhang Y, Liu L, Zhang G, Liu Z. Investigation of the influence of curing
494 temperature and silica fume content on setting and hardening process of the blended cement paste
495 by an improved ultrasonic apparatus. Constr. Build. Mater. 33 (2012) 32–40. DOI: 10.1016/
496 j.conbuildmat.2012.01.011
497 [41] Luna-Galiano Y, Fernández-Pereira C, Izquierdo M. Contributions to the study of porosity in
498 fly ash-based geopolymers. Relationship between degree of reaction, porosity and compressive
499 strength. Mater. Construcc. 66(324) (2016). http://dx.doi.org/10.3989/mc.2016.10215

500 [42] Rattanasak U, Chindaprasirt P. Influence of NaOH solution on the synthesis of fly ash
501 geopolymer. Miner. Eng. 22 (2009) 1073-1078. https://doi.org/10.1016/j.mineng.2009.03.022
502 [43] Olivares M, Laffarga J, Galán C, Nadal P. Evaluation of concrete mechanical strength through
503 porosity. Mater. Construcc. 54(273) (2004) 21-33. http://dx.doi.org/10.3989/mc.2004.v54.i273.220
504 [44] Provis JL, Van Deventer JSJ. Geopolymerisation kinetics. 1. In situ energy-dispersive X-ray
505 diffractometry. Chem. Eng. Sci. 62 (2007) 2309-2317. DOI: 10.1016/j.ces.2007.01.027
506 [45] Flores, P. Manual de acústica, ruidos y vibraciones. GYC (eds) (1990).
507 [46] Leiva C, Vilches LF, Arenas C, Delgado S, Fernández-Pereira C. Potential recycling bottom
508 and fly ashes in acoustic mortars and concretes. ACI Mater. J. 109(5) (2012) 529-536.
509 [47] Arenas C, Vilches LF, Leiva C, Alonso-Fariñas B, Rodríguez-Galán M. Recycling ceramic
510 industry wastes in sound absorbing materials. Mater. Construcc. 66(324) (2016) e059.
511 http://dx.doi.org/10.3989/mc.2016.10615.
512